LEARNING A VISUAL ATTENTION MODEL FOR ADAPTIVE FAST-FORWARD IN VIDEO SURVEILLANCE

Benjamin Höferlin[1], Hermann Pflüger[1], Markus Höferlin[2], Gunther Heidemann[3] and Daniel Weiskopf[2]

[1]*Intelligent Systems Group, University of Stuttgart, Stuttgart, Germany*

[2]*Visualization Research Center, University of Stuttgart, Stuttgart, Germany*

[3]*Computer Vision Group, Institute of Cognitive Science, University of Osnabrück, Osnabrück, Germany*

Keywords: Visual attention, Adaptive fast-forward, Video surveillance.

Abstract: The focus of visual attention is guided by salient signals in the peripheral field of view (bottom-up) as well as by the relevance feedback of a semantic model (top-down). As a result, humans are able to evaluate new situations very fast, with only a view numbers of fixations. In this paper, we present a learned model for the fast prediction of visual attention in video. We consider bottom-up and memory-less top-down mechanisms of visual attention guidance, and apply the model to video playback-speed adaption. The presented visual attention model is based on rectangle features that are fast to compute and capable of describing the known mechanisms of bottom-up processing, such as motion, contrast, color, symmetry, and others as well as top-down cues, such as face and person detectors. We show that the visual attention model outperforms other recent methods in adaption of video playback-speed.

1 INTRODUCTION

In video surveillance, operators are faced with huge amounts of surveillance footage. Due to unreliable automated video analysis, a common strategy to analyze surveillance videos is to watch the entire sequence (Höferlin et al., 2011). To save time, operators often accelerate the playback speed of the video. However, a typical property of surveillance footage is the nonuniform distribution of activity: busy periods alternate with idle periods. Since regular fast-forward plays the whole video at constant pace, operators are overburden during busy periods and bored during periods with no activity. A solution to alleviate this problem is to adapt the video playback speed according to the relevance of each frame: *adaptive fast-forward*. For video surveillance, two relevance measures are suggested in literature to evaluate the video content. (Peker and Divakaran, 2004) adapt the playback speed with respect to the motion and visual complexity present in a frame. In contrast to them, (Höferlin et al., 2011) measure the information gain (in terms of Shannon's information theory) between two successive frames by means of the symmetric Rényi divergence. Other adaptive fast-forward approaches (Petrovic et al., 2005; Cheng et al., 2009) are not adequate to surveillance applications because they utilize features (similarity to a target clip (Petrovic et al., 2005), manually defined semantic rules, and former playback preferences (Cheng et al., 2009)) that are not available in this context.

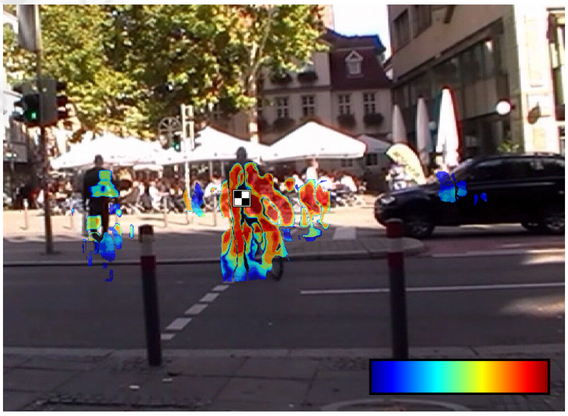

Figure 1: Saliency map calculated by the presented approach. Salient regions are illustrated by a color-coded overlay from blue (low saliency) to red (high saliency). The predicted fixation regions are compared to a real fixation (black/white box) recorded by an eye-tracker.

Höferlin B., Pflüger H., Höferlin M., Heidemann G. and Weiskopf D. (2012).
LEARNING A VISUAL ATTENTION MODEL FOR ADAPTIVE FAST-FORWARD IN VIDEO SURVEILLANCE.
In *Proceedings of the 1st International Conference on Pattern Recognition Applications and Methods*, pages 25-32
DOI: 10.5220/0003720000250032

In this paper, we introduce a novel *visual attention model* learned from fixation data captured by an eye-tracker. Based on this model, we predict the parts of surveillance videos that are likely to attract visual attention. Example prediction results for a single frame are depicted in Figure 1. We use these predictions to adapt the playback velocity of surveillance videos according to the visual saliency of the frames. Uninteresting parts are accelerated while periods that show high visual saliency are presented in slow-motion. Hence, the time required for analyzing a sequence as well as boredom are reduced while operators can keep track of relevant activities.

1.1 Visual Attention Models

The guided search model by (Wolfe, 1994) claims that attention is guided exogenous (i.e., based on the properties of visual stimuli; *bottom-up*) as well as endogenous (i.e., based on the demands of the observer; *top-down*). (Jasso and Triesch, 2007) explain in more detail that "bottom-up mechanisms are frequently characterized as automatic, reflexive, and fast, requiring only a comparatively simple analysis of the visual scene, top-down mechanisms are thought of as more voluntary and slow, requiring more complex inferences or the use of memory". According to Wolfe, early vision stages separate the visual stimuli into different feature maps. Each feature map contains a different feature channel, such as color, orientation, motion, or size. The feature maps are combined by a weighted sum into a single activation map, where the bottom-up activation represents a measure of how unusual a feature is compared to its vicinity (for each feature map). In contrast, the top-down activation emphasizes the features in which the subject is interested in (e.g., request for blue objects). The activation map determines which location receives attention (*winner-take-all* mechanism) and in which order: first the global maximum, then the second maximum, and so on (*inhibition-of-return*). The bottom-up activation does neither depend on the knowledge of the user nor on the search task.

Different visual attention models were developed to estimate the areas that attract attention. Most of these models are based on the bottom-up cues (Itti and Koch, 2001). One issue concerning such models is that these "saliency models do not accurately predict human fixations" (Judd et al., 2009). Therefore, learned models were proposed. For instance, (Judd et al., 2009) utilize a linear support vector machine to train a model of visual saliency including low-level (e.g., intensity, orientation, color contrast), mid-level (horizon line detector), and high-level features (face detector, people detector) to combine bottom-up signal cues and semantic top-down cues.

(Itti, 2005) presents an approach to calculate bottom-up saliency of video data. He collects eye-tracking data of subjects, and creates saliency maps using a computational model that considers low-level features. He further identifies that motion and temporal features are more important than color, intensity, and orientation. However, the best predictions are achieved by a combination of all these features. (Davis et al., 2007) train a focus-of-attention model to create pathways for PTZ (pan/tilt/zoom) cameras. Their model utilizes a single feature, translating motion, to capture the amount of activity. (Kienzle et al., 2007) train a feed-forward neural net with sigmoid basis functions. In their approach, the video is smoothed spatially and filtered temporally. Training of the neural net optimizes the temporal filters together with their weights. Another approach (Nataraju et al., 2009) combines a modified version of Kienzle's method with the visual attention model of (Itti et al., 1998), which is based on saliency maps. This approach uses a neural net to train the coefficients of three low-level descriptors (color intensity, orientation, and motion).

In contrast to the above mentioned methods, the model we introduce in this paper is not restricted to a single feature/channel (Kienzle et al., 2007), a saliency map from a single feature/channel (Davis et al., 2007), or a set of predefined channels (Nataraju et al., 2009). Our learning approach is based on temporal and spatial rectangle features and can thus represent rather arbitrary channels, such as lightness contrast, color contrast, motion, orientation, and symmetry. This means, we do not require manually modeled channels, we learn the bottom-up cues from training data. Further, the contribution of each feature to the final saliency map is determined by the training process. Hence, two important issues with channel-based saliency maps are addressed: the selection of features as well as their weights. Note that our approach also covers top-down mechanisms, such as the cues learned by (Judd et al., 2009): face and people detectors. Such high-level features are implicitly learned by our method. However, our approach does not consider the top-down mechanisms originating from memory effects.

The main contribution of this paper is the indication that visual attention (modeled by a classifier that is trained on eye-tracking data) is an excellent measure of relevance for adaptive video fast-forward. Further, we introduce a novel method to learn a visual attention model and show that this model is able to provide proper relevance feedback for surveillance video

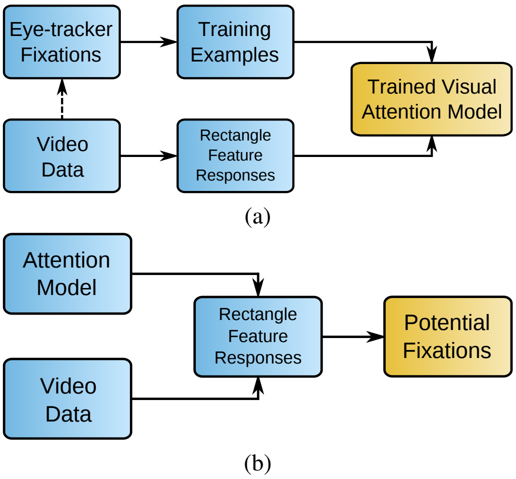

Figure 2: Schematic workflow of the training (a) and application (b) of our visual attention model. Arrows with solid lines show the workflow; the dashed line depicts the dependency between video and eye-tracking data.

data. Our experiments point out that the method introduced in this paper outperforms all other methods for playback-speed adaption in surveillance context. We show that our approach is robust to noise and that it is the only method that can cope with a combination of noise and low contrast (Section 3).

2 VISUAL ATTENTION MODEL

Our visual attention model mainly covers the bottom-up guidance of fixations, since we train it on the signal characteristics of real fixation points. We therefore call it memory-less, since it does only depend on the actual signal, but not on its history. This contrasts the memory-driven top-down guidance of visual attention of the human visual system. Hence, neither complex actions nor recall of objects could be explained by the presented model. However, this model is not completely free from top-down mechanisms, since the training data may also contain fixations guided by semantic meaningful objects. We do not distinguish between the original mechanisms (bottom-up or top-down) of the fixation data and are only concerned about their signal characteristics. Hence, fixations stemming from top-down guidance will affect our attention model. Examples of this issue are the facial regions included in the video data. Since faces are important in the context of video surveillance, the participants in our eye-tracker study sometimes focus on these regions during the collection of fixation data. These fixations do probably not stem from signal characteristics that attract attention, but from top-down mechanisms that suggest the semantic relevance of those regions. Thus, the attention model we train is to some extent also an object (or face) detector and responds to signal patterns of typical top-down mechanisms.

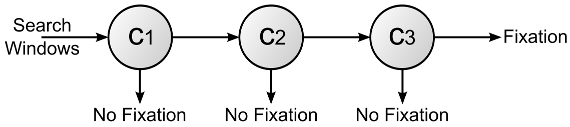

Figure 3: Cascade of three classifiers. Each classifier consists of multiple weak classifiers selected by Adaboost. The arrows depict the processing path of tested search windows.

Based on the video footage and the recorded fixation data, we create a discriminative visual attention model that consists of a cascade of classifiers. Figure 2 depicts the basic workflow of training and application of our visual attention model. Each classifier consists of a set of rectangle features (cf. Figure 4) selected by Adaboost (Viola and Jones, 2001). The cascade of boosted rectangle features became very popular for object detection, after it was successfully applied to face detection by (Viola and Jones, 2001). In particular, this approach is known for its fast computation utilizing an acceleration structure called *integral image* as well as cascaded classifiers with gradually increasing complexity. Classifiers at the beginning of the cascade are kept simple. Their goal is to inexpensively reduce the large amount of sliding windows that do not contain the searched object category, while preserving all windows with potential detections for the subsequent, more complex classifiers. Figure 3 displays such a cascade of classifiers. The decision H on the membership of a windowed video signal I_w to a particular class (fixation point or not) is calculated by each classifier using the sign-function of a weighted linear combination of N (thresholded) rectangle feature responses r_n and a bias b:

$$H(I_w) = \operatorname{sign}\left(\sum_{n=1}^{N} \alpha_n r_n(I_w) + b\right) \quad (1)$$

Training of a single classifier includes the selection of the appropriate rectangle features and their according weights α. These features are selected by Adaboost from a set of potential weak classifiers, i.e., rectangle features with a threshold. The types of available rectangle features were chosen carefully with respect to the causal mechanisms that are known to attract the visual attention of humans. By combining these features (main types are depicted in Figure 4), our model is able to represent more complex signal characteristics, such as lightness contrast, color

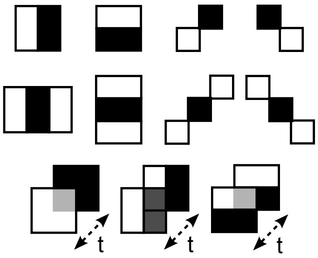

Figure 4: Basic types of rectangle features used to train the visual attention model. First row: spatial edge detectors. Second row: spatial ridge detectors. Third row: Temporal difference operator and spatio-temporal edge detectors. For visualization purposes, temporal rectangle features are depicted semi-transparent. Diagonal variants of the spatio-temporal edge detectors are not depicted, but used. Weak classifiers are created by thresholding nonuniformly scaled and translated instances (in all two/three dimensions) of these features. Features are calculated on the three dimensions of the CIE L*a*b* color space to incorporate color and lightness contrast.

contrast, motion, orientation, and symmetry. These signal characteristics represent the major cues for attention guidance according to (Itti, 2005) and (Wolfe, 1994). This means, our approach includes the typical categorical channels of bottom-up attention models based on saliency maps. However, it further solves the problem of selecting the individual weights of each channel by learning their contribution with respect to a particular class of stimuli (e.g., surveillance footage). Other approaches often require manual assignment of those weights. Further, our approach is capable of learning particular "channels" that have not been defined beforehand. While manually defined saliency operators need an exact definition of such channels, our method only requires a set of features that is able to cover these bottom-up cues. In this way, additional channels that are not explicitly mentioned here are learned from the data.

2.1 Fixation Data

To obtain examples required to train the visual attention model, we rely on fixation data from eye-tracking. We uses a *Tobii T60 XL* eye-tracker to record overt visual attention when free-viewing different stimuli. The training and test videos show outdoor environments at daytime and with continuous activity of pedestrians and/or cars, which are typical for video surveillance. Details of these video stimuli are listed in Table 1. We recorded eye-gaze data of 9 subjects for these videos. Fixations were filtered with the ClearView fixation filter using a velocity threshold of 20 px/ms and a duration threshold of 30 ms.

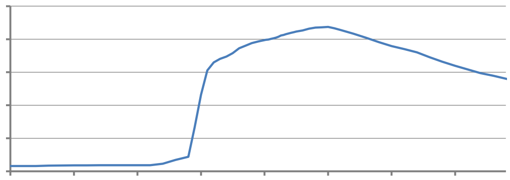

Figure 5: Performance of the visual attention model with respect to different threshold adaption values. In this experiment, the maximum shows a fixation prediction performance that is about 27 times above chance.

Outliers beyond the media borders were removed. Further, we excluded top-down-triggered fixations at points in the image that provide a good overview over the scene. These points (anchors) were frequently focused although no salient objects or actions were present. After further inquiry of the participants of the eye-tracker study, such anchor points could be identified to be mainly affected by top-down mechanisms employing knowledge, learned by watching the scene: at these strategic points, changes in the video were easily observed by peripheral vision. After filtering, in total 36717 fixations were left.

For the experiments, we use 70% of the fixation data for the training of the model, and the remaining 30% for analysis. The data is segmented in blocks of about 50 successive fixation points and the blocks selected for training/analysis are chosen equally distributed from the video. Positive examples are created using squared patches of 20 px, 40 px, 80 px, and 160 px side-length around the recorded fixation points. Negative training examples are generated with the same patch sizes at randomly (equally distributed) sampled positions in the video, but not within a spatio-temporal suppression radius around the fixations. All points within a weighted Euclidean distance of

$$d(P,N) = \sqrt{dx^2 + dy^2 + (\alpha dt)^2}$$

of less than 50 from a positive training example P are ignored in the selection of the negative training example N. Here, dx, dy, dt are the distances of the respective space and time dimensions (dx, dy measured in integer number of pixels, dt measured in integer number of time frames). A suitable value for the weight α was determined experimentally. For all evaluation results, we use $\alpha = 10$. The rationale behind the spatio-temporal suppression radius is to minimize the confusion between positive and negative examples by accounting for similar signal characteristics in the vicinity of fixations and for inaccuracy in the eye-tracking process.

Table 1: Different stimuli (progressive video footage) used to record fixation data.

Stimulus	Duration [frames/fps]	Resolution [pixels]	Compression	Example frame
S1	15825/25	1024×576	Microsoft Video 1 (CRAM)	
S2	15105/25	1024×576	Microsoft Video 1 (CRAM)	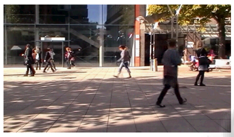
S3	15105/25	1024×576	Microsoft Video 1 (CRAM)	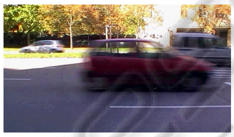
Intersection[1]	1355/25	640×480 (up-scaled)	Packed YUV4:2:2 (YUY2)	

However, there is no guarantee that a selected negative training example shows other signal characteristics than a positive example. It is also possible that a negative training example is a potential fixation point, but that it was not captured as such during the recording process, since too few samples were drawn from the distribution of fixations. This leads to bad linear separability of the training set. Hence, predefined classification goals as usually used for boosting (e.g., detection rate: 99% ; false positive rate: 30% as in (Viola and Jones, 2001)) and cascade construction are often not met. Therefore, we use a predefined number of classifiers with a predefined number of features per classifier for the training of the visual attention model, similar to (Zhao and Koch, 2011). All constants were determined empirically.

Finally, we adapt the thresholds b (cf. Eq. 1) of all classifiers. This step has direct influence on the area marked as potential fixation area by the learned visual attention model. Relaxation of the threshold leads to a generalization of the model and to more potential fixations, whereas increasing the threshold will reduce their amount. The adaption of the classifiers' thresholds is similar to the definition of a threshold for binarization of a saliency or activation map. Indeed, the trained focus-of-attention classifier can be regarded to maintain an intrinsic saliency map binarized according to the classifiers' thresholds. The saliency map depicted in Figure 1 is computed this way, by stacking several detection results with decreasing thresholds. Threshold adaption is further used in Section 3 to steer the playback-speed acceleration of adaptive fast-forward. We determine the optimal threshold adaption by applying gradient search on the *NSS* (*normalized scanpath saliency*) target function. Experiments suggest that this function shows almost concave behavior (see Figure 5) and, thus, can be optimized by gradient ascent with simulated annealing.

According to (Peters and Itti, 2007), NSS is defined as

$$NSS = \frac{1}{\sigma_M}(M(x,y) - \mu_M) \tag{2}$$

where (x,y) denotes the location of a recorded fixation and M represents the fixation map calculated by our visual attention model with the standard deviation σ_M and the mean μ_M.

2.2 Importance of Bottom-up Channels

The experiment shown in Figure 6 indicates a clear dependence between the performance of the learned visual attention model and the set of features used for selection by Adaboost. The chart illustrates the importance of the particular feature types. For instance,

[1]Concatenated videos from the CANDELA project: www.multitel.be/∼va/candela/intersection.html.

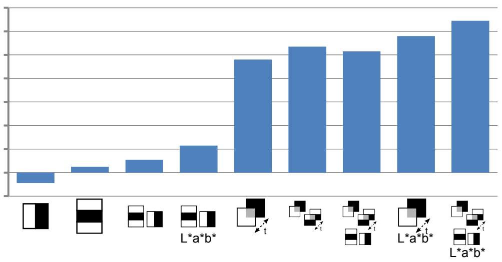

Figure 6: Performance of visual attention models trained with different sets of features. The principal type of features used in each experiment is depicted as surrogate beyond the particular bar. Rotational variants of the principal types are included in the training set. If features are calculated on all three color channels, the bar is labeled by L*a*b*, otherwise features are only calculated for the lightness channel.

a model that includes only simple edge/contrast detectors is not useful for the prediction of fixations in video. In the experiment, such a model is even worse than chance. Temporal features that describe the change of the lightness channel are most efficient. However, a combination of all features including color information shows best performance. These observations are consistent with the results of (Itti, 2005). Further, we find that the fraction of spatial features (56%) selected by Adaboost is slightly higher than the fraction of (spatio-)temporal features (44%). Feature selection by Adaboost further indicates that lightness (47%) and red/green opponent (35%) channels provide stronger cues than the yellow/blue channels (18%).

3 ADAPTIVE FAST-FORWARD

We apply the learned visual attention model to adaptive video fast-forward by calculating the area covered by potential fixation points as measure of a frame's relevance. The visual attention model we use in this experiment was trained on a heterogeneous video dataset different from the test dataset. The training dataset consists of 4 videos with different resolution, duration, and encoding (cf. Table 1). Additionally, perspective and captured objects vary from video to video. Hence, this experiment also indicates that the playback speed adaption using the presented visual attention model is to some extent insensitive to a specific training dataset. To improve robustness, we use fixations recorded from multiple subjects. The ratio of positive to negative examples was chosen 3:4, since experiments indicated slightly improved performance when more negative examples are used than positive examples.

We compare the performance of our method with the results of other relevance measures, such as motion activity (Peker and Divakaran, 2004) and Rényi divergence (Höferlin et al., 2011). The relevance feedback of these three methods calculated on the 4 video clips used in the user study of (Höferlin et al., 2011) is depicted in Figures 8 and 9.

Crowded Airport. *Night.*

Airport. *Noisy Airport.*

Figure 7: Example frames of the video sequences used for adaptive fast-forward experiments.

Three of the videos, termed *Crowded Airport*, *Airport*, and *Noisy Airport*, originate from the i-LIDS multi-camera tracking scenario. They are encoded with the Motion JPEG Video (MJPA) codec at a resolution of 720×576 px, and 25 fps. The *Noisy Airport* sequence is a version of the *Airport* sequence with added Gaussian noise. The *Night* sequence is an uncompressed monochrome video that was captured at night with a resolution of 656×494 px and 15 fps. The sequence includes regions with low contrast and dominant noise from high gain settings. Example frames of the videos are depicted in Figure 7. The results of the motion activity and Rényi divergence can be roughly summarized as follows (Höferlin et al., 2011):

- Motion activity and Rényi divergence perform well on *Crowded Airport* and *Airport* sequences.
- Motion activity fails to adapt the playback velocity of the *Noisy Airport* sequence, whereas Rényi divergence can cope with noise.
- Both methods are unable to adapt the playback speed of the *Night* sequence due to noise (motion activity) and low contrast (Rényi divergence).

Our method performs well for all four scenarios (cf. Figure 8 and 9). Especially, its performance in periods of no activity is remarkable. In these periods, the baseline of our method is consistently located

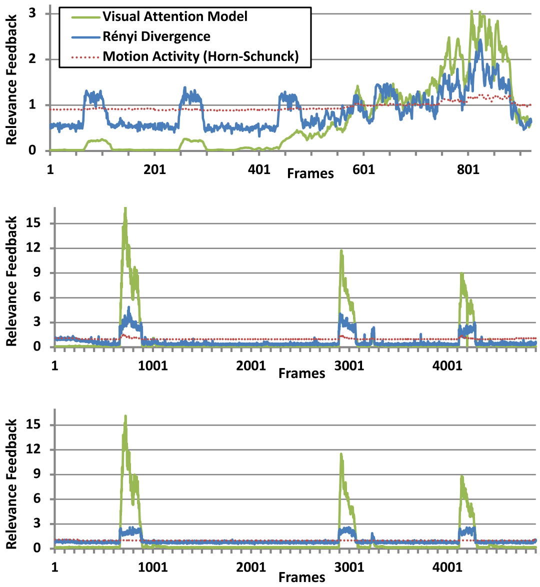

Figure 8: Relevance feedback of the compared methods (normalized to an expectation value of 1, i.e., the playback time of an accelerated sequence is the same for all methods, only acceleration of particular periods varies) for the sequences: *Crowded Airport* (top), *Airport* (center), and *Noisy Airport* (bottom).

close to zero relevance, as it is expected. In contrast to that, the other methods assign some amount of importance to these periods and especially the Rényi divergence jitters strongly around its baseline. Our visual attention model is also more robust to noise than the other methods. In fact, the Rényi divergence is robust to a certain degree, but a comparison of the relevance feedback of *Airport* (Figure 8 (center)) and *Noisy Airport* (Figure 8 (bottom)) indicates that our visual attention model better preserves the relevance signal under the influence of noise. Further, our approach is the only method that can cope with the high noise and low contrast scenario posed by the *Night* sequence. Figure 9 points out that only the visual attention model provides the expected result: high relevance at periods where people are present in the scene. Supplementary material that shows direct comparison of the different methods is available at our homepage[2].

4 CONCLUSIONS

We presented a novel method to learn a visual attention model that covers the main aspects of bottom-up processing, as well as some memory-less top-down

[2]www.vis.uni-stuttgart.de/index.php?id=1351

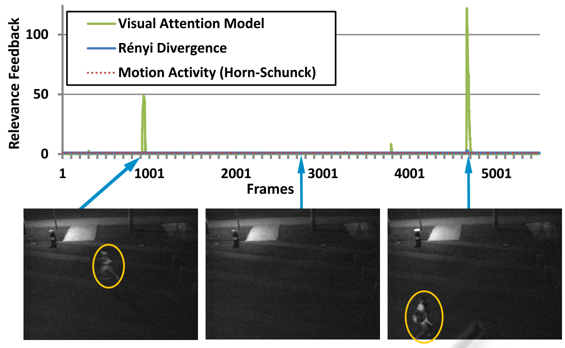

Figure 9: Relevance feedback of the compared methods (normalized to an expectation value of 1) for the *Night* sequence. Our visual attention model is the only approach that identifies relevant movement in this sequence with high noise and low contrast.

mechanisms. We were able to show that Adaboost is capable of training an effective model based on a rich set of rectangle features. In this way, the most important bottom-up channels for the attraction of visual attention were trained and represented by a weighted set of rectangle features. This model exhibits typical channel selection known from literature. Further, we applied our visual attention model to adaptive video fast-forward. In the evaluation using a dataset known from other approaches, our method outperforms the state-of-the-art and shows higher robustness to noise and low contrast. Future work includes a comprehensive evaluation of our visual attention model with respect to other visual attention models, and the generalization of the learned model to different stimuli, tasks, and subjects. Further fields of application of the visual attention model, such as video compression, video summarization, and adaptive camera switching could be considered in future work, too.

ACKNOWLEDGEMENTS

This work was funded by German Research Foundation (DFG) as part of the Priority Program "Scalable Visual Analytics" (SPP 1335).

REFERENCES

Cheng, K., Luo, S., Chen, B., and Chu, H. (2009). Smartplayer: user-centric video fast-forwarding. In *Proceedings of the International Conference on Human Factors in Computing Systems (CHI)*, pages 789–798. ACM New York.

Davis, J., Morison, A., and Woods, D. (2007). An adaptive focus-of-attention model for video surveillance and monitoring. *Machine Vision and Applications*, 18:41–64.

Höferlin, B., Höferlin, M., Weiskopf, D., and Heidemann, G. (2011). Information-based adaptive fast-forward for visual surveillance. *Multimedia Tools and Applications*, 55(1):127–150.

Itti, L. (2005). Quantifying the contribution of low-level saliency to human eye movements in dynamic scenes. *Visual Cognition*, 12(6):1093–1123.

Itti, L. and Koch, C. (2001). Computational modelling of visual attention. *Nature Reviews Neuroscience*, 2(3):194–203.

Itti, L., Koch, C., and Niebur, E. (1998). A model of saliency-based visual attention for rapid scene analysis. *IEEE Transactions on Pattern Analysis and Machine Intelligence*, 20(11):1254–1259.

Jasso, H. and Triesch, J. (2007). Learning to attend – from bottom-up to top-down. In Paletta, L. and Rome, E., editors, *Attention in Cognitive Systems. Theories and Systems from an Interdisciplinary Viewpoint*, volume 4840 of *Lecture Notes in Computer Science*, pages 106–122. Springer Berlin / Heidelberg.

Judd, T., Ehinger, K., Durand, F., and Torralba, A. (2009). Learning to predict where humans look. In *International Conference on Computer Vision*, pages 2106–2113. IEEE.

Kienzle, W., Schölkopf, B., Wichmann, F., and Franz, M. (2007). How to find interesting locations in video: a spatiotemporal interest point detector learned from human eye movements. In *Proceedings of the DAGM Conference on Pattern Recognition*, pages 405–414. Springer.

Nataraju, S., Balasubramanian, V., and Panchanathan, S. (2009). Learning attention based saliency in videos from human eye movements. In *Workshop on Motion and Video Computing (WMVC)*, pages 1–6. IEEE.

Peker, K. and Divakaran, A. (2004). Adaptive fast playback-based video skimming using a compressed-domain visual complexity measure. In *International Conference on Multimedia and Expo*, volume 3, pages 2055–2058.

Peters, R. and Itti, L. (2007). Beyond bottom-up: Incorporating task-dependent influences into a computational model of spatial attention. In *In Proceedings of Computer Vision and Pattern Recognition (CVPR)*, pages 1–8. IEEE.

Petrovic, N., Jojic, N., and Huang, T. (2005). Adaptive video fast forward. *Multimedia Tools and Applications*, 26(3):327–344.

Viola, P. and Jones, M. J. (2001). Robust real-time object detection. Technical Report CRL 2001/01, Cambridge Research Laboratory.

Wolfe, J. (1994). Guided search 2.0 a revised model of visual search. *Psychonomic Bulletin & Review*, 1(2):202–238.

Zhao, Q. and Koch, C. (2011). Learning visual saliency. In *In Proceedings of the Annual Conference on Information Sciences and Systems (CISS)*, pages 1–6.